RSC Advances

PAPER

View Article Online
View Journal | View Issue

Cite this: *RSC Adv.*, 2020, **10**, 689

Biocompatible supramolecular pseudorotaxane hydrogels for controllable release of doxorubicin in ovarian cancer SKOV-3 cells†

Caixia Li,[ab] Hanxue Li,[c] Jiahao Guo,[c] Liang Li,[c] Xiaowei Xi *[a] and Yanyan Yu*[c]

A series of injectable and biocompatible delivery DOX-loaded supramolecular hydrogels were fabricated by using presynthesized DOX-2N-β-CD, Pluronic F-127 and α-CD through host–guest interactions and cooperative multivalent hydrogen bonding interactions. The compositions and morphologies of these hydrogels were confirmed by PXRD and SEM measurements. Moreover, the Rheological measurements of these hydrogels were studied and the studies found that they showed a unique thixotropic behavior, indicting a fast self-healing property after the continuous oscillatory shear stress. Using α-CD as a capping agent, slow and sustained DOX release was observed at different pH values after 72 h. The amount of DOX released at pH 7.4 was determined to be 49.0% for hydrogel **1**, whereas the releasing amount of the DOX was increased to 66.3% for hydrogel **1** during the same period at pH 5.5 ($P < 0.05$), indicating a higher release rate of the drug under more acidic conditions. Taking hydrogel **1** as a representative material, the toxicities of DOX and hydrogel **1** on ovarian cancer cells (SKOV-3) at different exposure durations were examined. The results revealed that hydrogel **1** was less cytotoxic than free DOX to SKOV-3 cells ($P < 0.05$), suggesting sustained release by these hydrogels in the presence of ovarian cancer cells. It is anticipated that this exploration can provide a new strategy for preparing drug delivery systems.

Received 31st October 2019
Accepted 22nd December 2019

DOI: 10.1039/c9ra08986a

rsc.li/rsc-advances

1 Introduction

Ovarian cancer is one of the most common malignant tumors in women. Once detected, 70% of ovarian cancer reaches the advanced stage because of its hidden biological behaviors.[1,2] Currently, surgery, chemotherapy and radiotherapy are the basic methods for treating ovarian cancer. After surgery, chemotherapy is the most important treatment method, as it may heal the lesion and cure the disease. Except for some patients with stage IA and IB G1 ovarian cancer, patients with cancers at all other stages require chemotherapy.[3,4] However, some of the chemotherapeutic drugs that have been developed have problems such as low solubility, poor stability, propensity to multidrug resistance (MDR), poor tumor targeting, undesired impacts on healthy tissues, and local or systemic toxic side effects in cells, which can limit their clinical application.

In recent years, hydrogels of hydrophilic polymers have been constructed through hydrogen bonding, hydrophobic interactions, pi–pi interactions and electrostatic interactions, and these gels have been extensively applied in biological and medical fields because of their desirable elasticity, bioadhesion and biocompatibility properties.[5,6] Yang's group designed a paclitaxel hydrogel with a targeting function, in which folic acid was introduced into the gel system as a targeting group, and small molecular hydrogels were obtained by interlacing a three-dimensional network composed of uniform nanospheres. The drug loading of paclitaxel in this hydrogel reached 49.4%, which is higher than the package volume of many drug delivery systems.[7] Xu's team used cervical cancer cells overexpressing esterase to synthesize peptide molecules that are affected by esterase. These molecules can enter cells and self-assemble into nanometer fibers, and then the nanofibers can intertwine to form hydrogels, resulting in the death of cervical cancer cells.[8] However, these hydrogels, represented by amphiphilic small molecules, inevitably require a high temperature for gel formation, which restricts their application as carriers of macromolecular drugs (proteins, genes, *etc.*).

Cyclodextrin (CD) is a macrocyclic compound with good water solubility and biocompatibility; thus, it has received much attention for the specific binding of organic and biological substrates. Supramolecular hydrogels constructed from CDs have been widely used in environmentally responsive

[a]*Shanghai General Hospital of Nanjing Medical University, 100 Haining Road, Hongkou District, Shanghai, 200080, P.R. China. E-mail: xiaoweixi19@126.com*

[b]*Department of Obstetrics and Gynecology, Kunshan Traditional Chinese Medicine Hospital, 189 West Chaoyang Road, Jiangsu, 215300, P.R. China*

[c]*School of Chemical and Environmental Engineering of Shanghai Institute of Technology, 100 Haiquan Road, Shanghai 201418, P.R. China. E-mail: sshnhyyy@sit.edu.cn*

† Electronic supplementary information (ESI) available. See DOI: 10.1039/c9ra08986a

biomaterials and injectable drug carriers due to their mild preparation conditions, the facile regulation of the gelation process, their good degradability and thixotropicity, their ability to be tuned to increase their sensitivity to a resistant cell line, and their ability to be implanted *via* injection, which prevents surgical injury.[9,10] Li's group constructed an injectable supramolecular hydrogel material of polyethylene glycol/α-CD, and the drug loading and controlled release properties of this material were assessed.[11] During the preparation of the gel, the drug was embedded in the gel matrix *in situ* by being blending with a polymer, which greatly increased the drug loading in the gel carrier. Barar's group developed dual thermo- and pH-sensitive injectable hydrogels of chitosan/(poly(*N*-isopropylacrylamide-*co*-itaconic acid)), which were used for doxorubicin delivery in breast cancer.[12] Wu's group prepared bionic multilayer hydrogel capsules, which were applied to inhibit the burst release of doxorubicin.[13] Choi's group prepared a temperature- and pH-sensitive supramolecular hydrogel by grafting glucose onto polylysine/α-CD.[14] Cheng's group constructed a supramolecular polyvinyl alcohol dendrimer/α-CD hydrogel loaded with cisplatin that can control the release of anticancer drugs based on photothermal effects.[15] Ma's group prepared supramolecular hydrogels containing CD/PEG dendritic compounds, which were used as injectable vectors to transfect mmp-9 shRNA plasmids into hne-1 nasopharyngeal carcinoma cells in nude mice.[16] Currently, this type of supramolecular hydrogel is generally prepared based on α-CD or an α-CD derivative. Due to the high cost of the chemical modification of α-CD, applications of such supramolecular hydrogels are generally limited. Compared with α-CD derivatives, β-CD derivatives are more broadly applicable as pharmaceutical excipients because of their low production cost and convenient synthesis; moreover, α-CDs possessing small cavities can form inclusion complexes with poly(ethylene oxide) (PEO) polymer chains with high affinity, while β-CDs are more inclined to form inclusion complexes with poly(polypropylene oxide) (PPO) polymer chains.[17,18]

Pluronics (poly(ethylene oxide)–poly(propylene oxide)–poly(ethylene oxide) (PEO–PPO–PEO)) approved for clinical use by the Food and Drug Administration (FDA) are a class of low-toxicity triblock copolymers that undergo a sol–gel transition at physiological temperatures in aqueous solution.[19] Compared with other pluronics, Pluronic F127 gel has been shown to be an ideal candidate for a potential drug carrier for controlled release to tumor and surrounding tissue due to its unique reverse thermal gelation, high drug uptake capacity and gelling ability under physiological conditions at low concentrations.[20,21] The F127 injectable gel used for delivering a drug into the tumor has advantages over passive or other actively targeted therapies regardless of vascular status; therefore, it can provide accurate dosing without systemic toxicity.[22]

Doxorubicin (DOX), an antitumor antibiotic, can affect DNA base pairs and bind to DNA in cells, inhibiting the synthesis of DNA due to insurmountable obstacles and, as a result, inhibiting cell proliferation.[23] This drug has effects on a variety of tumors and is widely used to treat various cancers. It is one of the first-line drugs for the treatment of ovarian cancer. However, in clinical use, this drug has been shown to have important negative effects, such as cardiac toxicity, gastrointestinal reactions, hair loss and bone marrow suppression, which limit its clinical applications.[24,25] To reduce the toxic side effects and improve the curative effects of the chemotherapy drug doxorubicin and prevent drug resistance, researchers have made great efforts to change the dosage form of doxorubicin and increase its ability to target tumor tissues.[26,27] The introduction of doxorubicin into hydrogels has great potential in the field of drug delivery.

Herein, we grafted DOX groups onto β-CD along with water-soluble α-CD as capping and adhesive agents, and Pluronic F127 was used as an axle to construct a novel supramolecular pseudorotaxane hydrogel drug delivery system, which could help stabilize the prodrug before it reaches the target. This supramolecular hydrogel can release the loaded drug in a pH-controlled manner *in vitro*. Ovarian cancer SKOV-3 cells were applied to investigate the cytotoxic activities of the DOX released from the hydrogels. This work provides a new methodology for constructing drug delivery systems. A schematic illustration is shown in Scheme 1.

2 Experimental section

2.1 Materials

α-Cyclodextrin (α-CD), β-cyclodextrin (β-CD) were dried for 48 h in a vacuum oven before use, which was supplied by Aladdin Reagent Co., Ltd. (Shanghai, China). 1,3-Propanediamine (99%) was purchased from Shanghai Sinopharm Chemical Reagent Co., Ltd. Pluronic F-127 (98%) was purchase from Aladdin Reagent Co., Ltd. (Shanghai, China) and was dried under reduced pressure at 60 °C for 24 h. Doxorubicin hydrochloride (DOX·HCl, 99%) was supplied by Shanghai Sinopharm

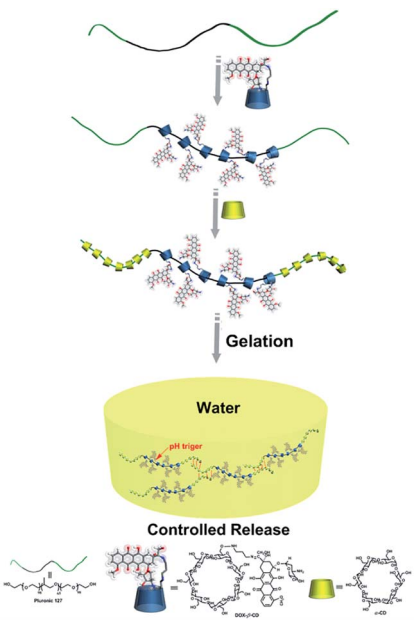

Scheme 1 The illustration of preparation of supramolecular DOX-loaded hydrogels.

Chemical Reagent Co., Ltd. All other reagents and solvents were of analytical grade and used as received without further purification. 6-Deoxy-6-OTs-β-CD was prepared according to the literature procedure.[28]

2.2 Synthesis of β-CD-propanediamine (2N-β-CD)[29]

Typically, dried 6-OTs-β-CD (1.6 mmol, 2 g) and 1,3-propanediamine (8 mmol 0.6 mL) were dissolved into anhydrous 1-methyl-2-pyrrolidinone (NMP, 41.5 mmol, 4 mL). Then, the reaction mixture was stirred at 80 °C for 10 h. After cooling to room temperature, the resulting solution was poured into anhydrous acetone (300 mL) with vigorous stirring, and the resultant mixture was stored in a refrigerator to produce a pale-yellow precipitate. The crude product was dissolved into a minimum of hot water (70 °C) and poured into acetone (300 mL). The white powder (1.6 g, 65% yield) was collected and dried under reduced pressure at 80 °C for 10 h. ^{1}H NMR (ppm, 500 MHz, D_2O, 298 K): δ 5.01 (s, 7H, H-1), 4.05–6.65 (m, 40H, H-3, H-5, H-6, H-2, H-4), 3.15 (m, 2H), 2.88 (m, 4H, –$NHCH_2$–), 2.72 (m, 2H, –CH_2–); FT-IR (KBr, ν cm^{-1}): 3368, 2936, 1560, 1456, 1274, 1123, 1013, 740, 751.

2.3 Synthesis of β-CD-propanediamine-DOX (DOX-2N-β-CD)

DOX-2N-β-CD was prepared according to a previously reported method.[30] DOX·HCl (0.7 mmol, 0.405 g) dissolved in CH_3OH (10 mL) and β-CD-propanediamine (0.4 mmol, 0.467 g) dissolved in 10 mL distilled water were combined in a 100 mL round bottom flask, and the reaction mixture was stirred at room temperature. One drop of trifluoroacetic acid was carefully added to the reaction system, and then the reaction mixture was stirred for another 48 h in the dark. The reaction progress was monitored by TLC, and then the reaction mixture was concentrated under reduced pressure. The resulting solid was dissolved into a small amount of DMSO and dropped into acetone (300 mL) with vigorous stirring, and the resultant mixture was stored in a refrigerator to produce a dark red precipitate. The above dissolution and precipitation process was repeated three times. Then, 0.57 g of red powder was collected and dried under vacuum for 12 h to yield 64% of the desired material.

2.4 Preparation of DOX-loaded supramolecular hydrogels[31]

In this study, supramolecular cyclodextrin pseudorotaxane hydrogels were prepared as listed in Table 1. Typically, different molar ratios of DOX-2N-β-CD were dissolved in water at 50 °C, then F127 was added. After the F127 was completely dissolved, the reaction was stirred for 1 h. Then different molar ratios of α-CD were added and the reaction was stirred for an additional 4 h at 50 °C to allow the formation of pseudorotaxane. The reaction mixture was then cooled to room temperature and allowed to gel for 12 h before the rheological studies. Similarly, blank hydrogel **1–6** were prepared with the same proportions to the corresponding hydrogel **1–6**. The details were shown in Table S1.† These hydrogels were freeze-dried and stored at 4 °C in the refrigerator. Each sample will be re-dissolved for experiments before use.

3 Characterization

3.1 ^{1}H NMR (500 MHz) spectra

^{1}H NMR (500 MHz) spectra were recorded on Bruker AVANCE III (500 MHz) spectrometer.

3.2 Fourier-transform infrared (FT-IR) spectra

Fourier-transform infrared (FT-IR) spectra were recorded using a Bruker Vertex 70 spectrometer. The samples for IR study were prepared as KBr pellets.

3.3 GPC measurements

Molecular weights and molecular weight distributions of prodrug hydrogels were determined by GPC at 35 °C using H_2O as the eluent (0.1 mol $NaNO_3$). The flow rate was 1 mL min^{-1}. A Waters 1515 series GPC system equipped with Waters 1515 Isocratic HPLC Pump, Ultrahydrogel 500 Pkgd column, and Waters 2414 Refractive Index Detector was used. Calibration was carried out using a series of poly(ethylene oxide) standards.

3.4 Sizes and zeta potentials

The sizes and zeta potentials of DOX-loaded supramolecular hydrogels were analyzed by the Zeta Potential Analyzer (Zetasizer Nano ZS 90, Malvern Instruments Ltd., UK).

3.5 Scanning electron microscopy (SEM)

Scanning electron microscopy (SEM) images were carried out on an FEI-Sirion 200 field-emission scanning electron microscope (FEI Co. with 20 kV operating voltage). Before measurement, the sample was sputter coated with gold.

Table 1 The composition for the DOX-loaded hydrogels

DOX-loaded hydrogels	α-CD	DOX-2N-β-CD	F127	DOX
1	20%[a]	1%[b]	5%[c]	1.12% (3.13 mg mL^{-1})
2	14.5%	2%	5%	2.91% (6.26 mg mL^{-1})
3	20%	3%	5%	3.36% (9.40 mg mL^{-1})
4	20%	4%	5%	4.48% (12.52 mg mL^{-1})
5	14.5%	4%	5%	5.83% (16.29 mg mL^{-1})
6	20%	8%	5%	8.96% (25.04 mg mL^{-1})

[a] w/v% of the saturated aqueous α-CD solution at 25 °C. [b] w/v% of DOX-2N-β-CD in a hydrogel. [c] w/v% of F127 in a hydrogel.

3.6 Transmission electron microscopy (TEM)

Transmission electron microscopy (TEM) measurements were performed on a JEOL JEM-2100F with accelerating voltage 200 kV.

3.7 X-ray diffractometer (XRD) measurements

Crystal structure identification of the samples was carried out using a PAN analytical Xpert Pro X-ray diffractometer (XRD) using Cu Kα radiation (λ = 0.154056 nm; Netherlands). The samples for XRD were supported on glass substrates.

3.8 Rheological measurements

Rheological measurements were performed on a stress-controlled Kinexus rheometer (Malvern instruments) with a 50 mm diameter parallel plate geometry and a measuring gap of 1 mm at 25 °C. All DOX-loaded supramolecular hydrogels were consolidated for 12 h at room temperature before the analysis. A strain amplitude sweep was conducted to ensure that experiments were done within the linear viscoelastic regime and a strain percent of 0.01% was selected. The dynamic modulus of the synthetic gel was recorded as a function of frequency (varying from 0.1 to 10 Hz). Results were averaged on three independent runs. Dynamic step-strain amplitude tests were performed by using 0.05% and 100% oscillation strain in each cycle at 1 rad s^{-1} angular frequency. The duration of strain at each step was 10 s.

3.9 Vitro drug release experiments

Vitro drug release experiments were performed as follows: different DOX-loaded supramolecular hydrogels were immersed in 2 mL PBS buffer solution (pH 7.4). These hydrogels were incubated at temperature to 37 °C with a shaking speed of 50 rpm, at regular intervals, 2 mL buffer solution was taken out, 2 mL of fresh buffer was add, the amount of released doxorubicin were determined through UV-vis spectrophotometer measured at 470 nm wavelength, the accumulation of drug release rate was used by the following formula:

$$Q = \frac{V_1 C_n + V_2(C_1 + C_2 + C_3 + \cdots + C_{n-1})}{m} \times 100\%$$

where, Q indicates the amount of DOX in the hydrogel, V_1 means the volume of the release medium, V_2 means the volume of sample, and n represents the concentration of DOX in the nth sample. All the release experiments were performed in triplicate, and the average results were presented.

3.10 *In vitro* cytotoxicity assay

Cell culture human ovarian carcinoma SKOV-3 cells were provided by the CTCC of Science (Shanghai, China). The cells were maintained in DMEM medium supplemented with 0.3 g L^{-1} L-glutamine, 3.7 g L^{-1} sodium bicarbonate, 10% heat-inactivated fetal bovine serum (FBS), penicillin (100 U mL^{-1}) and streptomycin (100 U mL^{-1}) in a humidified atmosphere of 5% CO_2, 95% air at 37 °C.

Cytotoxicity assay using MTT method serial dilutions of prodrug hydrogels were prepared by adding appropriate volume of the DOX-loaded hydrogel **1** solution to growth medium to yield different DOX concentrations ranging from 0.7 μg mL^{-1} to 5.6 μg mL^{-1}. Free DOX (dissolved in PBS solution containing 1.0% DMSO) and blank hydrogel were used as controls. Ovarian tumor cell SKOV-3 were transferred to the flat-bottomed 72-well culture plates (Corning, USA) at the density of 2, 000 cells per well 24 h prior to the assay. The culture medium in each well was carefully replaced with fresh medium containing serial dilutions of the DOX loaded hydrogel (the final concentration ranging from 62.5 μg mL^{-1} to 2767 μg mL^{-1}). After 72 h incubation at 37 °C and 5% CO_2, 20 μL of 5 mg mL^{-1} MTT (dissolved in PBS) was added to each well and the cells were incubated for another 4 h at 37 °C. The medium was removed and the dye was lysed with 200 μL DMSO. The absorption in each well was then measured at 570 nm using an automated Microplate Reader (Bio-Rad, USA), and the drug concentration that inhibited cell survival by 50% (IC_{50}) was determined from cell survival plots using Graphpad Prism 8.0. All the experiments were carried out in triplicates.

3.11 Statistical analysis

Statistical software SPSS 11.5 was used to analyse Comparison between different groups through one tailed Student's *t*-test. Data were represented as the mean values ± standard deviations. A p value less than 0.05 was considered statistically significant.

4 Results and discussion

4.1 Fabrication of the DOX-loaded hydrogels

To prepare the hydrogels, hydrophilic β-CD-propanediamine-DOX (DOX-2N-β-CD) segments were prepared first. Briefly, β-CD-OTs were first reacted with propanediamine to obtain a β-CD-propanediamine derivative (2N-β-CD), which was then condensed with DOX·HCl in the presence of a catalytic amount of trifluoroacetic acid to afford DOX-2N-β-CD. The Fourier transform infrared (FT-IR) spectrum (Fig. 1b) showed peaks near 1676 cm^{-1} and 1620 cm^{-1}, which can be attributed to carbonyl (C=O) and C=N stretching bands, confirming the formation of the DOX-2N-β-CD. As shown in Fig. 1a and S1a,† compared with the ^{1}H NMR spectrum of 2N-β-CD, the signals at 7.79, 7.75 and 7.54 ppm and two singlets at 3.93 and 1.15 were observed, which are assigned to the benzene groups and methyl

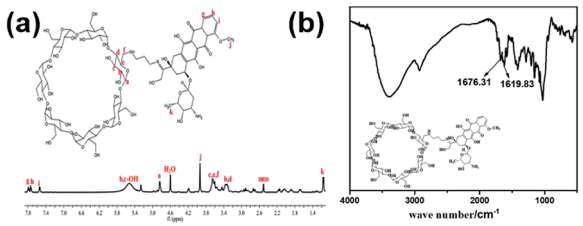

Fig. 1 ^{1}H NMR spectrum of DOX-2N-β-CD in DMSO-d_6 (a), FT-IR spectrum of DOX-2N-β-CD (b).

groups of the DOX moieties, respectively. These observations further confirm the successful synthesis of DOX-2N-β-CD. Based on the integrations of the ^{1}H NMR signals of the DOX and CD rings, two DOX moieties were grafted onto each β-CD; therefore, the drug content in DOX-2N-β-CD was 47.7%.

The DOX-loaded supramolecular hydrogels were prepared according to the previous method illustrated in Scheme 1. α-CD and β-CD can form inclusion complexes with PEG and PPG, respectively, and these inclusion complexes have necklace-like supramolecular structures.[18,32] The cavities of α-CD and β-CD are internally hydrophobic and externally hydrophilic, allowing them to bind to PEG and PPG chains through hydrophobic interactions. Therefore, the PEO segments of F127 can penetrate the α-CD cavities, whereas the PPO segments can penetrate the β-CD cavities, resulting in the formation of pseudorotaxane. Then, the poly-pseudorotaxane arrays interact to form supramolecular hydrogels *via* cooperative multivalent hydrogen bonding interactions.

The molecular weights and molecular weight distributions of DOX-loaded supramolecular hydrogels are shown in Table 2. It was shown that the hydrogel with a lower DOX content exhibited a shorter elution time than the hydrogel with a higher DOX content (Fig. S2†). The molecular weight distribution coefficients (M_w/M_n) of the hydrogels were determined to be from 1.018 to 1.030.

The sizes and zeta potentials of the DOX-loaded supramolecular hydrogels formed with different DOX contents were investigated, and the results are shown in Table 2. The sizes of the prodrug hydrogel obviously increased as the DOX ratio increased from 251.23 to 452.79 nm (Fig. S3†). Moreover, the zeta potentials of the hydrogels increased along with the DOX content from 10.02 to 20.28 (mV) (Fig. S4†).

Taking hydrogel **2** as an example, the morphology of DOX-2N-CD and the hydrogel **2** were determined from scanning electron microscopy (SEM) micrographs. As shown in Fig. 2, the DOX-2N-β-CD molecules were stacked in irregular blocks (Fig. 2a), while hydrogel **2** showed an interconnected porous structure with petal-like walls. The holes were heterogeneous and uneven in size and shape (Fig. 2b). TEM images showed a sheet structure with holes (Fig. S5†). The XRD pattern of the freeze-dried hydrogel powder showed two sharp peaks at $2\theta = 19.9^\circ$ and 22.5°, assigned to the {210} and {300} reflections, respectively, revealing that the PEO chains slide into the α-CD cavities and form inclusion complexes. In addition, the additional peak at $2\theta = 17.9^\circ$ indicates the formation of new ordered structures (Fig. 2c). This signal is likely due to the presence of

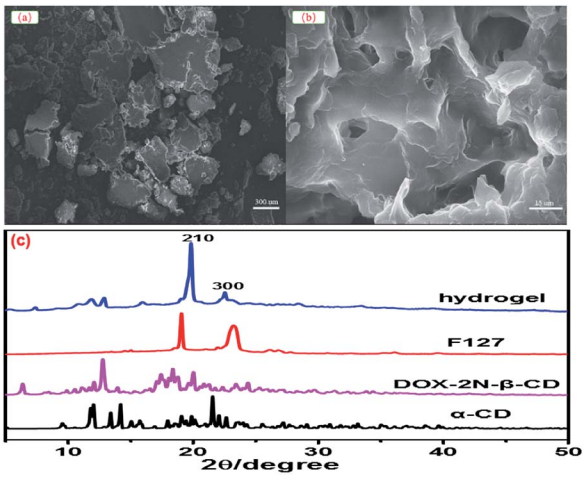

Fig. 2 SEM images of DOX-2N-β-CD (a) and DOX-loaded hydrogel **2** (b). Powder X-ray diffraction patterns for DOX-loaded hydrogel **2**, F127, DOX-2N-β-CD and α-CD (c).

secondary hydroxyl groups outside the α-CD, which could be further self-assembled into microcrystalline regions through hydrogen bonds. The scattering of light in these microcrystalline regions can be enhanced, resulting in the formation of an opaque hydrogel.

4.2 Rheological studies

To identify the viscoelastic properties of the DOX-loaded hydrogels, hydrogel **1–6** with different proportions of α-CD and DOX-2N-β-CD were selected for rheological experiments. As shown in Fig. 3, oscillation strain sweep experiments were used to determine the storage moduli, G' values, of the prodrug hydrogels at oscillation strains that were low yet larger than their loss moduli, G'' values. The elastic moduli of hydrogels are independent of the concentrations of α-CD and F127, suggesting that pseudorotaxane formation is the primary factor controlling the formation of the hydrogel. Hydrogel **2** possesses yield strains (where $G' = G''$) of 8%, at which point the non-covalent interactions are extensively disrupted. The yield strain decreased as the α-CD concentration increased. However, the yield strain did not obviously change when the DOX-2N-β-CD concentration was increased. These results suggest that increasing the α-CD concentration could effectively promote the formation of pseudorotaxanes and the subsequent formation of

Table 2 The GPC value, sizes and zeta potentials of DOX-loaded supramolecular hydrogels formed with different DOX content ($n = 3$)

DOX-loaded hydrogels	M_w	M_n	M_w/M_n	Zeta potential (mV)	Size (nm)
1	503 469	494 566	1.018	10.02 ± 0.9	251.23 ± 13.85
2	506 045	495 606	1.021	12.32 ± 1.1	298.80 ± 15.76
3	500 778	488 177	1.026	15.63 ± 0.8	349.78 ± 17.94
4	499 360	485 731	1.028	18.94 ± 1.4	399.45 ± 19.53
5	501 434	490 043	1.023	17.63 ± 1.0	301.27 ± 16.01
6	508 086	493 287	1.030	20.28 ± 1.3	452.79 ± 22.67

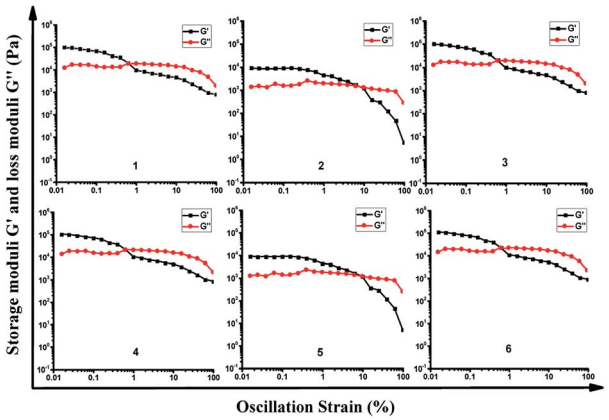

Fig. 3 Oscillation strain sweep profiles of DOX-loaded hydrogel **1–6**.

pseudorotaxane crystalline domains, which will deform at lower strains.

In the linear viscoelastic region, angular frequency sweep experiments were used to determine the elastic and loss moduli at room temperature (Fig. S4†). All DOX-loaded hydrogels exhibit frequency-independent moduli. The elastic properties of these hydrogels can be improved by increasing the concentration of α-CD, and the hydrogels are stable ($G' > G$) at different oscillation frequencies, suggesting that pseudorotaxane does not disassociate even at low frequencies.

To explore their injectability, the shear viscosities of the DOX-loaded hydrogels were investigated (Fig. S5†). The shear viscosities for all the hydrogels obviously decreased when the shear rate increased, which is consistent with the typical shear-thinning behavior of physically crosslinked hydrogels. Moreover, at the same shear rate, the shear viscosity of the supramolecular hydrogel increased upon increasing the α-CD concentration.

Dynamic step-strain amplitude experiments were applied to explore the self-healing of the supramolecular hydrogels. As shown in Fig. 4, the hydrogels **1–6** exhibited viscoelastic properties at the 0.05% strain. After applying stress to result in 100% strain, the viscoelastic properties of these hydrogels were decreased significantly. When the strain was returned to the 0.05% stain again after 200 s of the continuous stress, these hydrogels could partially recover their viscoelastic properties within 10 s. Among these supramolecular hydrogels, the G' was estimated to be approximately 80% of the initial G'. The observation suggested that the rapid recovery behavior of these hydrogels well indicated the thixotropic property based on the cooperative multivalent hydrogen bonding interactions.

Two weeks later, the stress stability tests at different temperatures were re-conducted. As shown in the Fig. S8,† the G' at 25 °C was estimated to be 99% of the G' two weeks ago, indicating that these hydrogels still persevered good thixotropic property. Though the G' at 37 °C was estimated to be approximately 92% of that at 25 °C in the Fig. S9,† even at 40 °C, the G' was measured to be about 85% of that at 25 °C (Fig. S10†), the stress stability tests also exhibited the rapid recovery behavior of these hydrogels, suggesting that thixotropic property would be a common property for these hydrogels at different temperatures.

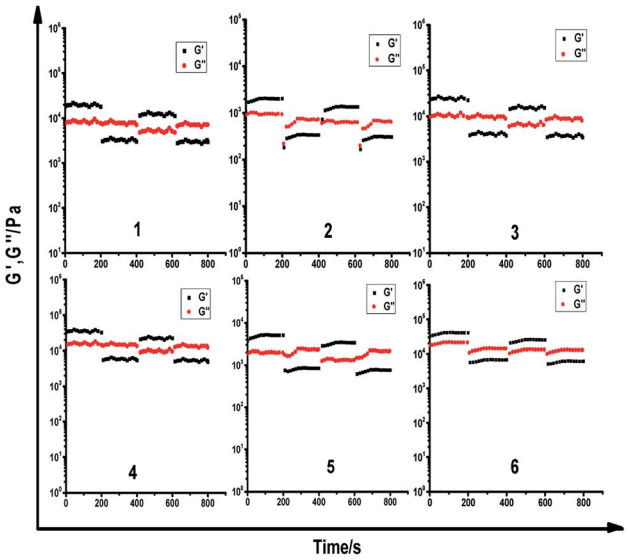

Fig. 4 Dynamic step strain amplitude test of hydrogels (γ = 0.05% or 100%).

The blank hydrogels were also performed *via* dynamic step-strain amplitude experiments (Fig. S11†). The results demonstrate that the blank hydrogels exhibited the similar thixotropic property to their corresponding DOX-loaded hydrogels.

4.3 *In vitro* drug release system

CD-based hydrogels have attracted increasing attention in efficient and precise drug delivery systems because of their good controlled and sustained release of drug molecules. Compared with the construction of non-covalent complexes *via* CDs and hydrophobic drugs, grafting DOX onto CDs can increase the solubility of hydrophobic drugs and ameliorate the undesirable effects of the drugs in many kinds of drug delivery systems.[33,34]

Unlike the traditional drug-loaded hydrogels, the DOX content in these supramolecular hydrogels was dependent on the amount of DOX-2N-β-CD.[30] To investigate the controllable release of DOX from hydrogel **1**, **4** and **6** with a gradient variation in DOX, the UV–vis spectra of these hydrogels were acquired to measure the amount of DOX released. Various pH values associated with pathological conditions are commonly applied to trigger the release of a drug into an organ with specific functions. Various anticancer drug delivery systems have exhibited differences between healthy tissues (pH 7.4) and the extracellular environment of solid tumors (pH 5.0–6.8).[35] As shown in Fig. 5a, the release profiles of DOX from the different hydrogels were determined at pH 7.4. As the DOX concentration increased from 3.13 to 25.04 mg mL^{-1}, the total cumulative release percentage was 10.77% for hydrogel **6**, and 20.99% for hydrogel **4** in 72 h, whereas the amount of DOX release was increased to 49.0% for hydrogel **1**, which was obviously higher than that at pH 7.4 ($P < 0.05$). Moreover, the amount of DOX release was increased to 15.56% for hydrogel **6** and 66.33% for

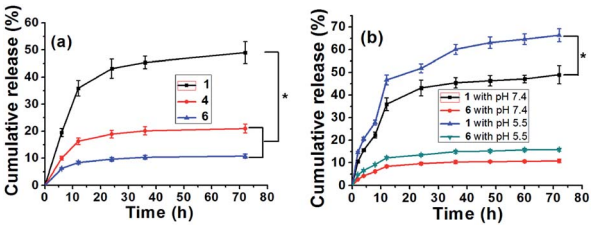

Fig. 5 The release of DOX from the hydrogel **1**, **4** and **6** *in vitro* (a), the data is shown as the mean ± SD ($n = 6$) with $^*P < 0.05$; the release of DOX from the DOX-loaded hydrogel **1** and **6** under different pH conditions (b). The data is shown as the mean ± SD ($n = 6$) with $^*P < 0.05$.

hydrogel **1** during the same period at pH 5.5 ($P < 0.05$). Two weeks later, the release profiles of DOX from the hydrogel **1** and **6** were re-determined at different pH in 72 h, respectively. As shown from the Fig. S12,† the total cumulative release percentage was 48.5% for hydrogel **1** and 10.66% for hydrogel **6** at pH 7.4, respectively. Whereas the amount of DOX release was increased to 65.3% for hydrogel **1** and 15.4% for hydrogel **6** at pH 5.5, which was similar to the releasing amount of DOX from the hydrogel **1** and **6** two weeks ago, demonstrating the stability of these hydrogels. The above observations suggest a higher release rate of the drug under more acidic conditions (Fig. 5b). This trend may occur because the C=N bond in the DOX-2N-β-CD is sensitive to acid and is more likely to break at a lower pH, resulting in a higher release rate. However, the advantage of the DOX-loaded hydrogels for the pH-sensitive release is not obvious. Some reasonable explanations are as follows: first, the swelling effect of the hydrogel may accelerate in an acidic solution, resulting in drug release behavior in hydrogels.[12,36] However, many α-CDs as capping agents can trap DOX in the gel, decreasing the rate of drug release from the hydrogels. Second, the different DOX loading concentrations can influence the release behavior of hydrogels. In comparison to the hydrogel containing a higher drug content, the hydrogel with a lower drug content exhibited a higher initial dramatic release as well as a higher release rate.[13] It was expected that the drug release response of this pH-sensitive supramolecular hydrogel may decrease the negative effects of the drug and reduce the cytotoxicity of the drug to healthy cells.

4.4 *In vitro* cytotoxicity assay

The cytotoxic activities of DOX-loaded hydrogels were investigated using human ovarian tumor cells (SKOV-3) in an MTT assay with a test concentration of 5 mg mL^{-1} and an incubation time of 72 h. As shown in Fig. 6 and S13,† the blank hydrogel and 1.0% DMSO in PBS showed no cytotoxicity, and the hydrogel **1** showed less cytotoxicity toward SKOV-3 cells than free DOX solution with increasing DOX concentrations from 0.7 μg mL^{-1} to 5.6 μg mL^{-1} ($P < 0.05$). This result reveals that the DOX-loaded hydrogels allow significant sustained release of the drug to the sensitive SKOV-3 cells.

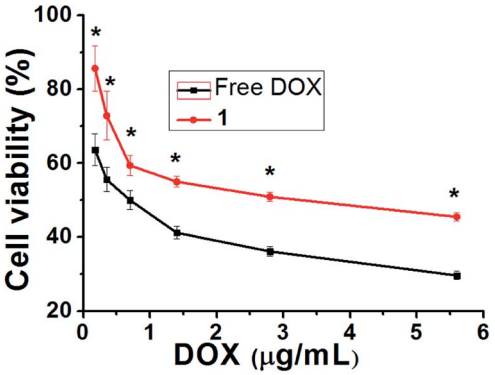

Fig. 6 Comparison of cytotoxicity between DOX and hydrogel **1** against ovarian carcinoma cells. The data is shown as a mean ± SD ($n = 3$) with $^*P < 0.05$.

5 Conclusion

In this study, we prepared a novel type of injectable and biocompatible hydrogel for drug delivery, and the gel was formed by DOX-2N-β-CD, F-127 and α-CD through host–guest interactions and cooperative multivalent hydrogen bonding interactions under mild conditions. The PXRD and rheological measurements showed that the DOX-loaded hydrogels were successfully prepared. These hydrogels show the high gelation ability and stability by primarily controlled by the α-CD content. Fast recovery property of these hydrogels were obtained after mechanical stress at different temperature. These hydrogels exhibit pH-dependent DOX release. At normal pH (7.4), the amount of DOX released was determined to be 49.0%, whereas at pH 5.0, up to approximately 66.33% of DOX could be released. Taking DOX-loaded hydrogel **1** as an example, hydrogel **1** exhibited lower cytotoxicity than free DOX in SKOV-3 cells. The supramolecular hydrogel developed herein could provide an efficient platform for designing drug delivery systems.

Conflicts of interest

The authors have no conflicts of interest to declare for this communication.

Acknowledgements

The authors acknowledge the National Science Foundation of China (NSFC) (No. 21502116) and the Development Program of Kunshan Science and Technology (KS1550).

Notes and references

1 J. Barbier, X. Chen, G. Sanchez, *et al.*, An NF90/NF110-mediated feedback amplification loop regulates dicer expression and controls ovarian carcinoma progression, *Cell Res.*, 2018, **28**(5), 556–571.

2 A. Padmanabhan, N. Candelaria, K. K. Wong, *et al.*, USP15-dependent lysosomal pathway controls p53-R175H turnover in ovarian cancer cells, *Nat. Commun.*, 2018, **9**(1), 1270.
3 R. Haag and F. Kratz, Polymer therapeutics: concepts and applications, *Angew. Chem., Int. Ed.*, 2006, **45**, 1198–1215.
4 Y. F. Fu, C. Y. Zhou, X. Li, *et al.*, The inhibition of UBC13 expression and blockage of the DNMT1-CHFR-Aurora a pathway contribute to paclitaxel resistance in ovarian cancer, *Cell Death Dis.*, 2018, **9**, 93.
5 A. Shekaran, J. R. Garcia, A. Y. Clark, *et al.*, Bone regeneration using an alpha 2 beta 1 integrin-specific hydrogel as a BMP-2 delivery vehicle, *Biomaterials*, 2014, **35**(21), 5453–5461.
6 K. Yue, G. Trujillo-de Santiago, M. M. Alvarez, *et al.*, Synthesis, properties, and biomedical applications of gelatin methacryloyl (GelMA) hydrogels, *Biomaterials*, 2015, **73**, 254–271.
7 H. Wang, C. Yang, L. Wang, *et al.*, Self-assembled nanospheres as a novel delivery system for taxol: a molecular hydrogel with nanosphere morphology, *Chem. Commun.*, 2011, **47**, 4439–4441.
8 Z. Yang, K. Xu, Z. Guo, *et al.*, Intracellular enzymatic formation of nanofibers results in hydrogelation and regulated cell death, *Adv. Mater.*, 2007, **19**, 3152–3156.
9 L. Yin, S. X. Xu, Z. J. Feng, *et al.*, Supramolecular hydrogel based on high-solid-content mPECT nanoparticles and cyclodextrins for local and sustained drug delivery, *Biomater. Sci.*, 2017, **5**, 698–706.
10 L. Dai, K. F. Liu, L. Y. Wang, *et al.*, Injectable and thermosensitive supramolecular hydrogels by inclusion complexation between binary-drug loaded micelles and α-cyclodextrin, *Mater. Sci. Eng., C*, 2017, **76**, 966–974.
11 J. Li, X. Li, X. Ni, *et al.*, Self-assembled supramolecular hydrogels formed by biodegradable PEO–PHB–PEO triblock copolymers and a-cyclodextrin for controlled drug delivery, *Biomaterials*, 2006, **27**, 4132–4140.
12 M. Fathi, M. Alami-Milani, M. Hossein Geranmayeh, *et al.*, Dual thermo-and pH-sensitive injectable hydrogels of chitosan/(poly(N-isopropylacrylamide-co-itaconic acid)) for doxorubicin delivery in breast cancer, *Int. J. Biol. Macromol.*, 2019, **128**, 957–964.
13 W. Zhang, X. Jin, H. Li, *et al.*, Onion-structure bionic hydrogel capsules based on chitosan for regulating doxorubicin release, *Carbohydr. Polym.*, 2019, **209**, 152–160.
14 H. S. Choi, K. Yamamoto, T. Ooya, *et al.*, Synthesis of poly(ε-lysine)-grafted dextrans and their pH- and thermosensitive hydrogelation with cyclodextrins, *ChemPhysChem*, 2005, **6**, 1081–1086.
15 X. Wang, C. Wang, Q. Zhang, *et al.*, Near infrared light-responsive and injectable supramolecular hydrogels for on-demand drug delivery, *Chem. Commun.*, 2016, **52**, 978–981.
16 Q. Lin, Y. Yang, Q. Hu, *et al.*, Injectable supramolecular hydrogel formed from a-cyclodextrin and PEGylated arginine-functionalized poly(L-lysine) dendron for sustained MMP-9 shRNA plasmid delivery, *Acta Biomater.*, 2017, **49**, 456–471.
17 A. Harada, J. Li and M. Kamachi, The Molecular Necklace: a rotaxane containing many threaded α-cyclodextrins, *Nature*, 1992, **356**, 325–327.
18 M. Rekharsky and Y. Inoue, Complexation Thermodynamics of Cyclodextrins, *Chem. Rev.*, 1998, **98**, 1875–1917.
19 E. Gioffredi, M. Boffito and S. Calzone, Pluronic F127 hydrogel characterization and biofabrication in cellularized constructs for tissue engineering applications, *Procedia CIRP*, 2016, **49**, 125–132.
20 Z. Yang, W. L. Hsiao, W. Pam and S. Nie, Thermoreversible Pluronic F127-Based Hydrogel Containing Liposomes for the Controlled Delivery of Paclitaxel: In Vitro Drug Release, Cell Cytotoxicity, and Uptake Studies, *Int. J. Nanomed.*, 2011, **6**, 151–166.
21 F. S. Schanuel, K. S. Raggio Santos, A. Monte-Alto-Costa and M. G. de Oliveira, Combined Nitric Oxide-Releasing Poly(vinyl alcohol) Film/F127 Hydrogel for Accelerating Wound Healing, *Colloids Surf., B*, 2015, **130**, 182–191.
22 N. L. Elstad and K. D. Fowers, OncoGel (ReGel/paclitaxel) – clinical applications for a novel paclitaxel delivery system, *Adv. Drug Delivery Rev.*, 2009, **61**, 785–794.
23 J. C. Wang, DNA topoisomerases, *Annu. Rev. Biochem.*, 1996, **65**, 635–692.
24 J. S. Choi, K. O. Doh, B. K. Kim, *et al.*, Synthesis of cholesteryl doxorubicin and its anti-cancer activity, *Bioorg. Med. Chem. Lett.*, 2017, **27**, 723–728.
25 B. Vincenzi, M. Frezza, D. Santini, *et al.*, New therapies in soft tissue sarcoma, *Expert Opin. Emerging Drugs*, 2010, **15**, 237–248.
26 L. Wu, D. Leng, D. Cun, *et al.*, Advances in combination therapy of lung cancer: Rationales, delivery technologies and dosage regimens, *J. Controlled Release*, 2017, **260**, 78–91.
27 Y.-P. Fan, J.-Z. Liao, Y.-Q. Lu, *et al.*, MiR-375 and Doxorubicin Co-delivered by Liposomes for Combination Therapy of Hepatocellular Carcinoma, *Mol. Ther.–Nucleic Acids*, 2017, **7**, 181–189.
28 L. Li, H. Y. Zhang, J. Zhao, *et al.*, Self-sorting of four organic molecules into a heterowheel polypseudorotaxane, *Chem.–Eur. J.*, 2013, **19**(20), 6498–6506.
29 T. Sun, M. Ma, H. Yan, *et al.*, Vesicular particles directly assembled from the cyclodextrin/UR-144 supramolecular amphiphiles, *Colloids Surf., A*, 2013, **424**, 105–112.
30 Y. Wang, H. Wang, Y. Chen, *et al.*, Biomimetic pseudopolyrotaxane prodrug micelles with high drug content for intracellular drug delivery, *Chem. Commun.*, 2013, **49**, 7123–7125.
31 Q. Lin, X. Hou and C. Ke, Ring Shuttling Controls Macroscopic Motion in a Three-Dimensional Printed Polyrotaxane Monolith, *Angew. Chem., Int. Ed.*, 2017, **56**, 4452–4457.
32 J. Li, X. Li, X. Ni, *et al.*, Self-assembled Supramolecular Hydrogels Formed by Biodegradable PEO-PHB-PEO Triblock Copolymers and α-Cyclodextrin for Controlled Drug Delivery, *Biomaterials*, 2006, **27**, 4132–4140.
33 J. T. Zhang, S. W. Huang, J. Liu and R. X. Zhuo, Temperature Sensitive Poly[N-isopropylacrylamide-co-(acryloyl β-

cyclodextrin)] for Improved Drug Release, *Macromol. Biosci.*, 2005, **5**, 192–196.

34 S. Salmaso, A. Semenzato, S. Bersani, *et al.*, Cyclodextrin/PEG Based Hydrogels for Multi-Drug Delivery, *Int. J. Pharm.*, 2007, **345**, 42–50.

35 J. Zhao, G. Jin, G. Weng, J. Li, J. Zhu and J. Zhao, Recent advances in activatable fluorescence imaging probes for tumor imaging, *Drug Discovery Today*, 2017, **22**(9), 1367–1374.

36 J. Qu, X. Zhao, P. X. Ma and B. Guo, pH-responsive self-healing injectable hydrogel based on N-carboxyethyl chitosan for hepatocellular carcinoma therapy, *J. Colloid Interface Sci.*, 2019, **536**, 224–234.